Influence of Zeolite Catalyst Supports on the Synthesis of Single-Walled Carbon Nanotubes: Framework Structures and Si/Al Ratios

Takahiko Moteki,[1,†] Daiki Nukaga,[1] Yoichi Murakami,[2] Shigeo Maruyama,[3] and Tatsuya Okubo,[1]*

[1]Department of Chemical System Engineering, The University of Tokyo, 7-3-1 Hongo, Bunkyo-ku, Tokyo 113-8656, Japan

[2]Department of Mechanical Sciences and Engineering, Tokyo Institute of Technology, 2-12-1-I1-15 Ookayama, Meguro-ku, Tokyo 152-8552, Japan

[3]Department of Mechanical Engineering, The University of Tokyo, 7-3-1 Hongo, Bunkyo-ku, Tokyo 113-8656, Japan

KEYWORDS: Support material; SWNT; catalytic CVD; metal catalyst; Zeolite

ABSTRACT: Choice of the catalyst support is an important factor for the synthesis of single-walled carbon nanotubes (SWNTs) by the catalytic chemical vapor deposition (CCVD) method. Zeolites, which are a class of microporous crystalline material, have also been known as the catalyst support for the synthesis of SWNTs. However, detailed influences of their porous framework and framework composition have not been clarified yet. In this study, we have

investigated zeolites as catalyst supports on the SWNTs synthesis. Various zeolites possessing different Si/Al ratios and framework types, FAU, *BEA, and MFI-type, were used as catalyst supports. Both properties influenced the SWNT growth, and the results are explained by the diffusion of catalyst metal atoms into the zeolite framework and the stabilization of the diffused atoms at ion-exchange sites in the crystals. By tuning these properties, zeolites could be convenient catalyst supports that can impart relatively wide effective loading range to the metal catalyst for the CCVD growth of SWNTs.

INTRODUCTION: Single-walled carbon nanotubes (SWNTs) have attracted considerable attention due to their unique properties promising for many applications.[1] Metal oxides have been used as catalyst supports because of their high thermal and chemical stability. Dense oxides such as quartz and alumina have been widely used for the carbon nanotubes (CNTs) synthesis by the catalytic chemical vapor deposition (CCVD) method. On the other hand, porous materials such as zeolite and mesoporous silica also have been known as useful catalyst supports.[2–13] In the typical CCVD method, SWNTs are grown from supported metal nanoparticles by being exposed to gas-phase carbon sources at elevated temperatures (600–800 °C). Under high temperature, aggregation and/or Ostwald ripening lead to an increase of the metal nanoparticle diameter.[14–18] The diameter of SWNT is strongly correlated with the diameter of the metal nanoparticles, and SWNTs are not grown from the metal nanoparticles if their size is either too large or too small. Thus, the interaction between the metal catalyst and oxide support surface is one of the factors that influence the SWNT growth, and it is important to choose a proper support that can provide optimal metal nanoparticles. In this sense, the selection and/or design of the support material has been an important issue.

Among zeolites, a USY zeolite (FAU-type structure) has often been employed as a useful catalyst support due to its high thermal and chemical stability.[1–3,6–8] Zeolites are a class of microporous crystalline aluminosilicates, and over 200 distinct frameworks having unique void and pore structure are presently known.[19] The unique porous framework structure is expected to positively influence on SWNT synthesis.[1–3,6–8,20] However, the detailed influence of the zeolite has not been sufficiently clarified, and researchers have paid less attention to it. Moreover, only limited types of zeolites have been commercially available from suppliers. For the advanced use of zeolites as support materials, further understanding is required.

Recently, an atomically flat surface of siliceous zeolite, *b*-plane of silicalite-1 (MFI-type structure), was investigated as a model zeolitic catalyst support for SWNT synthesis.[20] The study showed that the deposited metal atom diffused into the zeolite crystal under a reductive environment at high temperature CCVD process, and the diffused metal was considered to be incorporated into the zeolite framework.[20] Generally, zeolites have lower density than other high density oxides used in the SWNT synthesis, such as amorphous silica glass, quartz, alumina, and sapphire.[21] It was concluded that the diffusion of the metal atom into the zeolite supports was originated from their low density and porous structure.[20] However, the previous study only focused on the siliceous MFI-type zeolite, and it is inadequate to cover the variety of zeolites. Therefore, systematic studies are required to understand the influence of zeolite properties, such as framework structures and chemical compositions (silicon to aluminum ratio, Si/Al ratio).

In this study, we have investigated the influence of framework types and Si/Al ratios of zeolites on the SWNT synthesis by using several zeolites as catalyst supports. Three types of zeolite frameworks possessing different framework densities, FAU, *BEA, and MFI, have been employed (Table 1). The framework density influenced the diffusivity of the metal atom into the

zeolite support, and the diffused metal atoms would be strongly interacted with Al sites in the framework. By selecting the proper zeolite support, SWNTs were grown over two orders of magnitude concentration of metal dipping solution.

Table 1. Properties of zeolite frameworks

Framework type	Framework density (T-atom/nm^3)[a]	Pore structure
FAU	13.3	3 dimensional
*BEA	15.3	3 dimensional
MFI	18.4	3 dimensional

[a]Tetrahedral atom (Si and Al)

EXPERIMENTAL

Zeolite preparation. H^+-aluminosilicate FAU-type zeolites (HSZ-390HUA, HSZ-385HUA, HSZ-360HUA, and HSZ-320HOA) were supplied from Tosoh Corporation. *BEA-type zeolites were synthesized according to previous literature.[22,23] In the synthesis of aluminosilicate *BEA-type zeolites, the atomic Si/Al ratio of the reactant gels were adjusted to 100, 50, and 10. MFI-type zeolites were synthesized according to the previous literature.[24] In the synthesis of aluminosilicate MFI-type zeolites, the Si/Al ratio of the reactant gels were adjusted to 30 and 15. All the synthesized products were collected by filtration and washed with distilled water, followed by calcination at 773 K for 5 h with a muffle oven to remove the included organics. Because MFI-type aluminosilicate zeolites contained sodium cations, they were ion-exchanged with ammonium nitrate, and then calcined at 773 K for 5 h to prepare H^+-form samples.

Catalyst supporting. Cobalt catalysts were supported by dipping the zeolite crystals into the cobalt acetate solution. Each zeolite sample was ground with a mortar and then dispersed in distilled water. Then, the dispersion liquid was dropped on a Ti-coated (50 nm) Si substrate. It was then heated at 773 K for 5 h to fix the zeolite crystals on the substrate. They were dipped in an aqueous cobalt acetate tetrahydrate [$Co(OAc)_2 \cdot 4H_2O$] solution at 0.10, 0.25, 0.75, 2.5, 5.0, and 10 wt. % concentrations for several minutes. Finally, the substrates were heated at 773 K for 5 h to remove the acetate species.

SWNT synthesis. SWNTs were synthesized by alcohol CCVD method using a procedure described in the previous literature.[3,4] Briefly, the substrates were placed in a quartz tube held inside an annular electric furnace. After evacuation, the furnace was heated up to 1073 K and the content of the tube was exposed to a flowing gas mixture of Ar/H_2 (3% H_2) at 40 kPa to reduce the oxidized cobalt. After the furnace reached 1073 K, a holding time of 10 min (also called pre-reduction time) was imposed before introducing ethanol vapor (carbon source) into the quartz tube. Ethanol vapor was then passed through the quartz tube at 0.31 kPa for 30 s without a carrier gas. SWNTs were only grown on the surfaces of zeolite crystals because the cobalt that deposited on the surface of the Ti-coated substrates was deactivated by the Ti layer at 1073 K.

Characterization. The structures of the prepared zeolites were examined with a powder X-ray diffractometer (XRD; M03X-HF, Bulker AXS) using Cu Kα radiation over a range of 5°–45° (2 θ). The chemical composition analysis of the zeolites was performed by an inductively coupled plasma-atomic emission spectrometer (ICP-AES; iCAP 6300, Thermo Scientific) after dissolving the sample in a KOH solution. The morphology of the zeolite crystals and the synthesized SWNTs was observed using a field-emission scanning electron microscope (SEM; S-4800,

Hitachi) at a low accelerating voltage of 1 kV. SWNTs were also characterized by a microscope Raman scattering spectroscopy system (excitation wavelength: 488 nm).

RESULTS

Characterization of Prepared Zeolite Crystals

Four FAU-type (with Si/Al ratio = 2.9, 6.7, 48, and 410), four *BEA-type (with Si/Al ratio = 10, 25, 99, and pure silica), and three MFI-type zeolite samples (with Si/Al ratio = 16, 45, and pure silica) were investigated. The Si/Al ratio of the synthesized zeolite crystals was confirmed by ICP-AES measurements. The representative XRD patterns of prepared zeolite samples are shown in Figure 1. All the peaks from each sample are explained in terms of FAU, *BEA, and MFI-type frameworks, and no byproducts nor amorphous phases were observed. To test the stability against the CCVD process, all the zeolite samples were subjected to a pseudo-CVD process (see Supporting information, Figure S1), which is a CCVD process without deposition of the metal catalyst (no SWNTs generation). The thermal stability of zeolites generally decreases with the decrease of Si/Al ratio. However, in this study, the zeolite sample with the lowest Si/Al ratio maintained its framework structure after the pseudo-CVD process (Figure 1). The SEM observations indicated that the pseudo-CVD process did not change the morphology of the crystals. Thus, all the prepared zeolite samples could be applied as the stable supports. This result made us doubt the widely believed idea that high Si/Al ratio zeolites are preferred for CCVD growth substrates because of their higher thermal stability. It should be noted that the whole CCVD process completed within 1 h (about 50 min of temperature elevation and 10 min of holding time), which is much shorter than the stability test usually performed on zeolites.

Moreover, the CCVD process proceeded under dry condition without being exposed to water vapor. Therefore, the dealumination and the decomposition of the zeolites were mostly hindered.

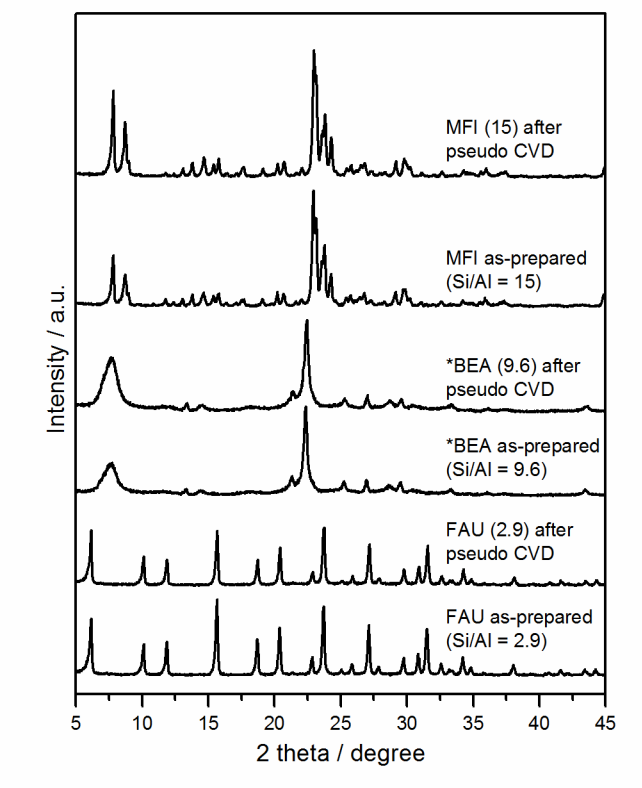

Figure 1. XRD patterns of the prepared zeolite samples possessing the lowest Si/Al ratios and the same samples subjected to the pseudo-CVD process.

Characterizations of the synthesized SWNTs

Figures 2 and 3 show the representative Raman spectra and SEM images of SWNTs, respectively, synthesized on the zeolite samples possessing the highest Si/Al ratios using the 2.5 wt. % of cobalt solution. The prominent peak at 1593 cm^{-1} is the G-band (named after graphite) peak and the peak around 1350 cm^{-1} is the D-band (named after defect) peak (Figure 2).[25] The high G-band to D-band ratio implies that the synthesized SWNTs are highly graphitized. The sharp peak at 520 cm^{-1} observed in the FAU and *BEA-type zeolites spectra is associated with

the silicon substrate (Figures 2a and 2b). In the case of MFI-type zeolites, a strong background due to zeolite luminescence was observed.[21] Several weaker peaks observed around 150–300 cm^{-1} are from the radial breathing mode (RBM) corresponding to the axial-symmetric radial vibration, which indicates SWNTs (inserted in Figure 2).[25] It is widely accepted that the peak position of RBM is correlated to the diameter of SWNTs.[25] However, the distribution of RBM peaks significantly varies with the excitation wavelength, and the intensity strongly depends on both diameter and chirality of the SWNT.[26,27] Therefore, only a rough estimation of diameter distribution could be possible with single laser excitation, as described below. The bright lines observed in the SEM images are bundles of SWNTs or isolated SWNTs (Figure 3). The SWNTs were randomly oriented and abundantly grown, indicating that the metal catalyst particles were well dispersed on the zeolite crystals.

Figure 4 shows the dependence of the G-band intensities on the cobalt concentrations. Typical Raman spectra of SWNTs synthesized on zeolite crystals with the highest Si/Al ratio are shown in Supporting Information (Figures S2–S4). The G-band intensity could be used as a primitive guide to roughly estimate the relative amount of collective SWNTs as a first approximation.[28] Because Raman scattering from SWNTs is a resonance process,[29–31] if a sample investigated has a specific or discontinuous distribution in diameter or chirality, it would be highly inappropriate to use G-band intensity as a quantitative measure for comparing relative mass yields of SWNTs. However, as recognized by the RBM spectra (Figures 2 and S2–S4), the present samples do not have a particular selectivity on the chirality. Additionally, the diameter distribution is thought to be broad and continuous to some extent, based on the aspects that (i) all the RBM spectra are broad and highly poly-component, and (ii) the RBM spectral shapes look similar with each other. Therefore, we think that estimations of relative SWNT mass yields using the G-band intensity

would be allowed in the first approximation for the present case. On the basis of Raman spectra and SEM images, we also confirmed that the G-band intensity was correlated with the amount of SWNTs. Although this is an approximate method to estimate the quantity of SWNTs, it is mentioned that the G-band originates from an existence of graphitized carbon species, and especially, that the G-band around 1590 cm^{-1} originates from graphitized SWNTs.[25,32] Furthermore, it has been previously shown that the G-band intensity correlates well with the amount of SWNTs directly evaluated by photograph and high-resolution SEM images.[14,28] In addition, the amount of the zeolites and the weight ratio between the zeolite and the SWNTs are too small to be evaluated by more accurate quantification methods such as a thermo-gravimetric analysis. Because of these, we rely on the G-band intensity in this article.

As shown in Figure 4, the concentration of cobalt acetate varied from 0.1 to 10 wt. %. The plotted marks in Figure 4 represent the averaged values of the G-band intensities from eight measurements performed on the same sample. Each vertical bar attached to a mark represents the data scattering range (1 standard deviation). In the case of FAU-type zeolites, at the Si/Al ratios of 2.9 and 6.7, the G-band intensities were very low or they were not observed in the Raman spectrum regardless of the cobalt concentration, indicating that SWNTs were rarely grown. On the other hand, at the Si/Al ratios of 48 and 410, the average G-band intensities of the obtained SWNTs were remarkably higher. They increased with the increase of cobalt concentration and reached a maximum at 10 wt. % (Figure 4a). In the case of *BEA-type zeolites (Figure 4b), at the Si/Al ratio of 25, the average G-band intensities were negligible in the concentration range from 0.1 to 2.5 wt. %. However, they apparently increased with increasing cobalt concentration (to 5 wt. %). At the Si/Al ratio of 99, G-band intensities were slightly higher than that at the Si/Al ratio of 25 over all the concentration range. In the case of pure silica, they were apparently

high and reached a maximum at 5 wt. % (Figure 4b). In the case of MFI-type zeolites, the average G-band intensity was remarkable for the case of the pure silica form, and it reached a maximum at 5 wt. % (Figure 4c). Almost no SWNTs were grown on the zeolite samples at Si/Al ratios of 15 and 43 in the lower concentration below 2.5 wt.%. Regardless of the framework types, SWNTs growth is favored on zeolite samples with high Si/Al ratios.

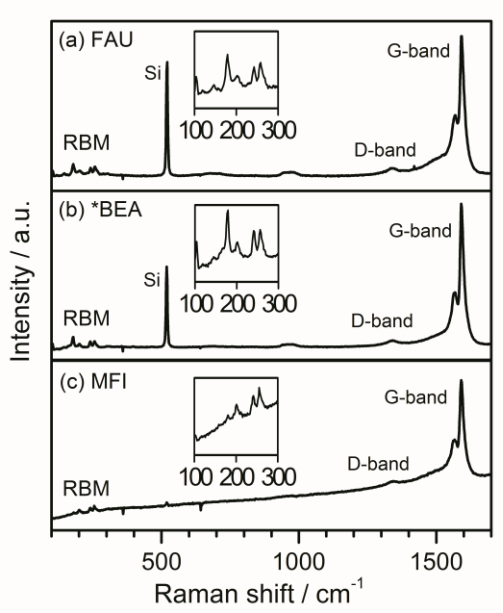

Figure 2. Typical Raman spectra of SWNTs synthesized on (a) FAU (Si/Al = 410), (b) *BEA (pure silica), and (c) MFI-type zeolite crystals (pure silica). A cobalt acetate tetrahydrate solution (2.5 wt. %) was used for catalyst loadings.

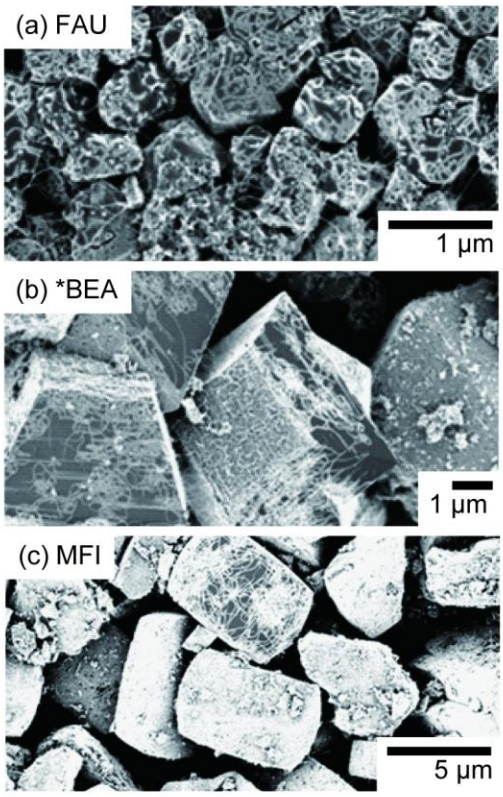

Figure 3. Typical SEM images of SWNTs synthesized on (a) FAU (Si/Al ratio = 410), (b) *BEA (pure silica), and (c) MFI-type zeolite crystals (pure silica). A cobalt acetate tetrahydrate solution (2.5 wt. %) was used for catalyst loadings.

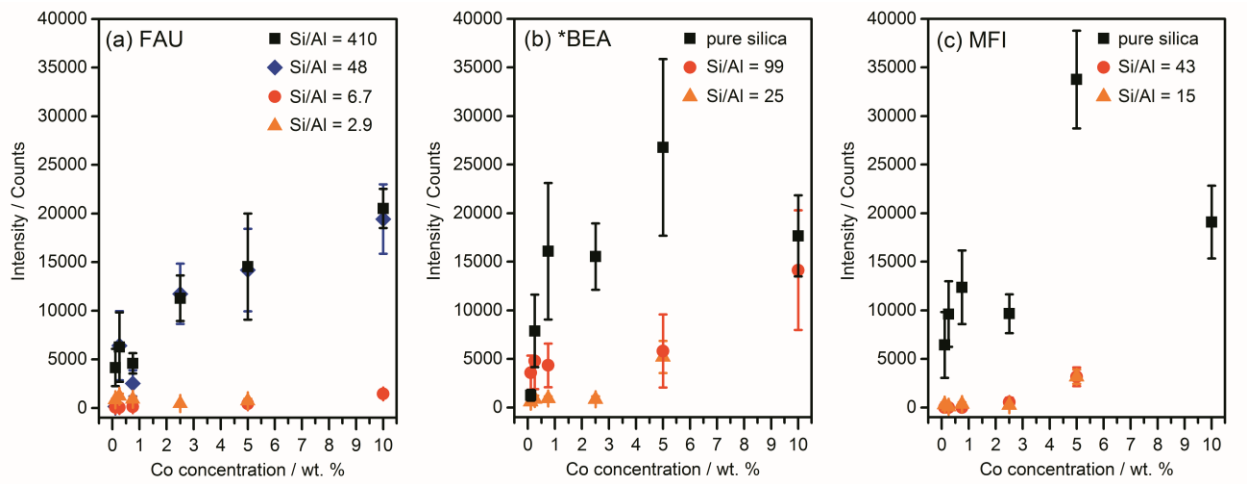

Figure 4. Dependence of the G-band intensities on the concentration of the cobalt acetate tetrahydrate solution for the (a) FAU-type, (b) *BEA-type, and (c) MFI-type zeolite crystals with different Si/Al ratios.

DISCUSSION

As mentioned above, SWNTs have been catalytically grown from metal nanoparticles formed by thermal aggregation and/or Ostwald ripening. The optimal size of the metal nanoparticle is essential to catalyze the formation of SWNTs, because too large or too small particles do not catalyze it.[28] In this study, metal deposition is done by simple method; dipping zeolite crystals into aqueous solution. Such a solution-based technique, due to the capillary action of cobalt solution between zeolite particles, may not control the amount of metal precisely compared to high-vacuum deposition technique such as sputtering. However, we did not observe any obvious spotty generation of SWNTs. Moreover, it should be noted that the SWNTs were generated from wide concentration range from 0.1 to 10 wt.% (i.e. two orders of magnitude wide) by selecting the suitable zeolite such as FAU-type zeolite with Si/Al ratio of 410. This may indicate that wide SWNT synthesis condition (allowable catalyst loading range) is accepted compared to the cases where dense and non-porous substrates were used, and this could be a unique characteristic of zeolite support.

The influence of the density of the zeolite support was clarified by comparing zeolite samples possessing different framework types at the same Si/Al ratio. We selected the highest Si/Al ratio crystals as representative samples, such as aluminosilicate FAU-type zeolites with the Si/Al ratio of 410 and pure silica *BEA and MFI-type zeolites. Although the aluminosilicate FAU-type zeolite crystal contained small amounts of framework Al atoms (Si/Al ratio = 410), it could be

considered as a siliceous type zeolite. As shown in Table 1, the framework densities of FAU, *BEA, and MFI-type zeolites were 13.3, 15.3, and 18.4 T-atom/nm^3, respectively, indicating that their densities were approximately 1.3, 1.5, and 1.8 g/cm^3, respectively. The G-band intensities of *BEA and MFI-type zeolites were maximized at lower concentration (5 wt. %) than that of FAU-type zeolite at 10 wt. % (Figure 4). Therefore, the amount of metal atom to form optimal size metal nanoparticles was lower in *BEA and MFI-type zeolites than that in FAU-type zeolite. This difference could be explained in terms of framework density of the zeolite. The framework density of FAU-type zeolite is lower than that of the other two frameworks (Table 1). Our previous work revealed the diffusion of metal atoms into the zeolite support under CCVD process, and strong interaction between cobalt atom and zeolite framework was demonstrated by X-ray photoelectron spectroscopy.[20] Thus, zeolites could be regarded as a "sponge" for excess metal atoms. In this sense, more amounts of metal atoms could diffuse into the zeolite with lower framework density during the CCVD process. And, more amounts of metal atoms would be necessary to form proper size nanoparticles. Compared to FAU-type sample, oversized nanoparticles would be formed on *BEA and MFI-type samples at the concentration of 10 wt. %, because the diffusion of the metal is relatively weak, due to their denser frameworks. This result suggests that the size of the metal nanoparticles formed on the zeolite surface could be controlled by tuning the framework density of the zeolite support.

The influence of the Si/Al ratio was analyzed in each framework type. SWNTs were rarely generated on zeolite crystals with low Si/Al ratios (less than about 20) regardless of the framework type (Figure 4). This result can be explained in terms of the ion-exchange capacity of the zeolite. In the aluminosilicate zeolite, the negative charge of the framework AlO_2^- is generally compensated by the counter cation. In this study, the counter cations of all the prepared

aluminosilicate zeolites were protons. Ion-exchange between protons and cobalt cations could easily proceed in our process, and the cobalt atoms could strongly interact with the framework and be stabilized at the ion-exchange sites. In other words, the ion-exchange sites could capture the diffused cobalt atoms inside the zeolite crystals. The number of sites is proportional to the number of framework Al atoms, therefore samples with low Si/Al ratio have higher capacity for cobalt cations than those with high Si/Al ratios. Moreover, the interaction between the cations and the negatively charged aluminosilicate framework is stronger than that in neutral siliceous frameworks. Thus, excess metal atoms are required to form proper sized nanoparticles on the aluminosilicate zeolites compared to siliceous zeolites. The influence of Si/Al ratios seems to be more remarkable than that of the framework density.

In this study, the size of the obtained metal nanoparticles has been influenced by the two factors, which are the framework density (geometric factor) and the Si/Al ratio (chemical factor). We suggested that the framework density of zeolite would change the diffusivity of metal atom, and the Al sites in the zeolite framework would have strong interaction with the diffused metal atoms. This is schematically described in Figure 5.

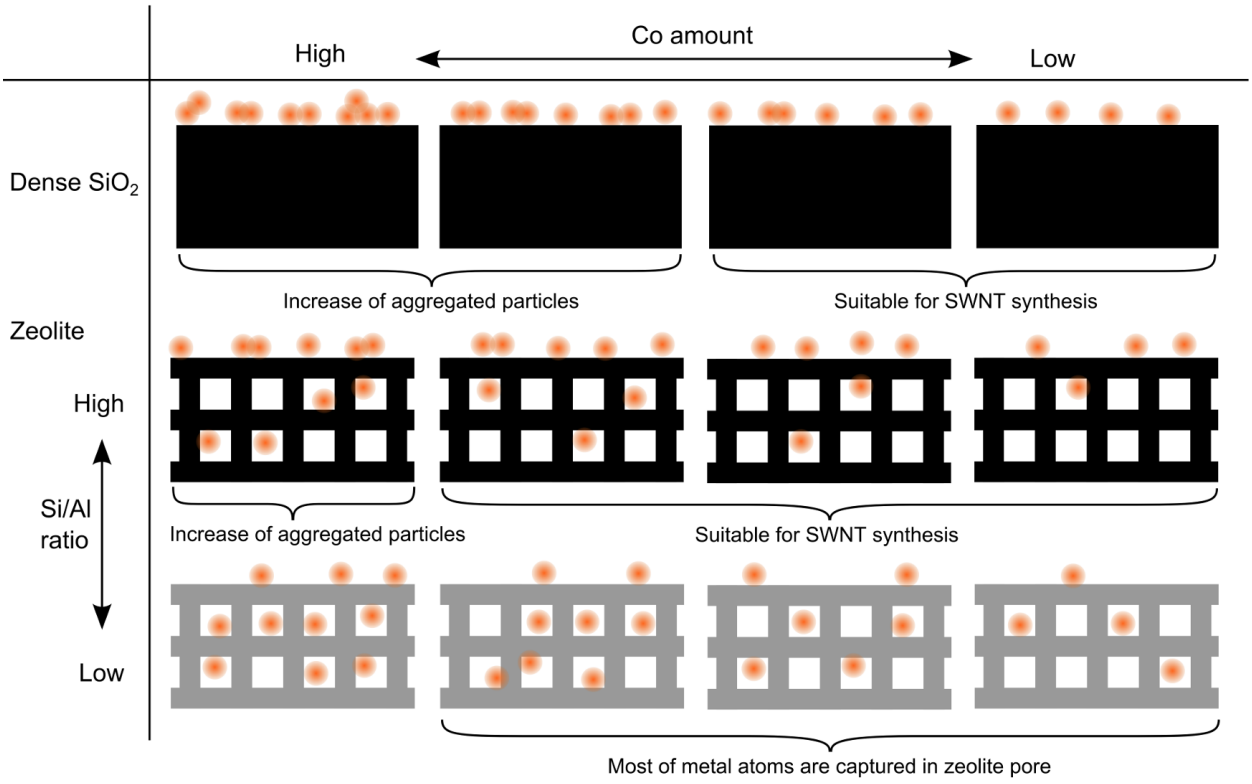

Figure 5. Schematic description of zeolite support in comparison to dense SiO_2 support.

CONCLUSIONS

The effect of a zeolite as a support material on SWNTs growth was investigated using an alcohol CCVD method on FAU, *BEA, and MFI-type zeolites possessing various Si/Al ratios. The deposited metal particles catalyze the SWNTs growth. At the same time, some of the metal atoms could diffuse into the zeolite crystals because of their porous framework structure. We demonstrated that both the framework density and the Si/Al ratio of the zeolites affected on the SWNTs growth. With the decrease of the framework density, the metal diffusion into the zeolite crystals would become easy and more metal was required to form nanoparticles with proper size to catalyze SWNTs on the crystal surface. The increase of Al sites in the framework resulted in the increase of ion-exchange sites where metal atoms are strongly captured as inactive species,

and it affected the SWNTs growth more remarkably. Interestingly, due to the zeolite properties, SWNTs were synthesized from a wide concentration range of metal dipping solution. The acceptable catalyst amount was largely relaxed by selecting the suitable zeolite. These are the unique characteristics of zeolite supports originated from their microporous structures.

ASSOCIATED CONTENT

Supporting Information. Powder XRD patterns of zeolites and Raman spectra of synthesized SWNTs. This material is available free of charge via the Internet at http://pubs.acs.org.

AUTHOR INFORMATION

Corresponding Author

*E-mail: okubo@chemsys.t.u-tokyo.ac.jp.

Present Addresses

†Center for Catalytic Science and Technology, Department of Chemical and Biomolecular Engineering, University of Delaware, 150 Academy Street, Newark, Delaware 19716, U. S. A. E-mail: moteki@udel.edu.

Notes

The authors declare no competing financial interest.

ACKNOWLEDGMENT

This work was supported by Grants-in-Aid for JSPS Fellows by the Japan Society for the Promotion of Science (JSPS) for Young Scientists. T. M. was JSPS research fellows and grateful to JSPS for Research Fellowships for Young Scientists. A part of this work was financially supported by Grant-in-Aid for Scientific Research (22226006, 25630063, 25107002) and IRENA Project by JST-EC DG RTD, Strategic International Collaborative Research Program, SICORP. The authors thank Dr. S. Noda (Waseda University) for easy access to a Ti sputtering system and useful discussions.

REFERENCES

1. Dresselhaus, M. S.; Dresselhaus, G.; Avouris, P. Carbon Nanotubes; Springer: Berlin, Germany, **2001**.

2. Okamoto, A.; Kawakubo, T.; Hiraoka, T.; Okazaki, T.; Sugai, T.; Shinohara, H. Synthesis and Characterization of Multi- and Single-Wall Carbon Nanotubes by the Catalytic Vapor Deposition Method. *Mol*. *Cryst*. *Liq*. *Cryst*. **2002**, *387*, 93–98.

3. Maruyama, S.; Kojima, R.; Miyauchi, Y.; Chiashi, S.; Kohno, M. Low-Temperature Synthesis of High-Purity Single-Walled Carbon Nanotubes from Alcohol. *Chem*. *Phys*. *Lett*. **2002**, *360*, 229–234.

4. Murakami, Y.; Miyauchi, Y.; Chiashi, S.; Maruyama, S. Characterization of Single-Walled Carbon Nanotubes Catalytically Synthesized from Alcohol. *Chem*. *Phys*. *Lett*. **2003**, *374*, 53–58.

5. Dai, H.; Rinzler, A. G.; Nikolaev, P.; Thess, A.; Colbert, D. T.; Smalley, R. E. Single-Wall Nanotubes Produced by Metal-Catalyzed Disproportionation of Carbon Monoxide. *Chem*. *Phys*. *Lett*. **1996**, *260*, 471–475.

6. Murakami, Y.; Yamakita, S.; Okubo, T.; Maruyama, S.; Single-Walled Carbon Nanotubes Catalytically Grown from Mesoporous Silica Thin Film. *Chem*. *Phys*. *Lett*. **2003**, *375*, 393–398.

7. Hiraoka, T.; Kawakubo, T.; Kimura, J.; Taniguchi, R.; Okamoto, A.; Okazaki, T.; Sugai, T.; Ozeki, Y.; Yoshikawa, M.; Shinohara, H. Selective Synthesis of Double-Wall Carbon Nanotubes by CCVD of Acetylene Using Zeolite Supports. *Chem*. *Phys*. *Lett*. **2003**, *382*, 679–685.

8. Kishi, N.; Kikuchi, S.; Ramesh, P.; Sugai, T.; Watanabe, Y.; Shinohara, H. Enhanced Photoluminescence from Very Thin Double-Wall Carbon Nanotubes Synthesized by the Zeolite-CCVD Method. *J*. *Phys*. *Chem*. *B* **2006**, *110*, 24816–24821.

9. Tamura, M.; Kemmochi, Y.; Murakami, Y.; Chino, N.; Ogura, M.; Naik, S. P.; Takai, M.; Tsuji, Y.; Maruyama, S.; Okubo, T. Synthesis of Single-Walled Carbon Nanotubes in Mesoporous Silica Film and Their Field Emission Property. *Appl*. *Phys*. *A* **2006**, *84*, 247–250.

10. Ramesh, P.; Okazaki, T.; Sugai, T.; Kimura, J.; Kishi, N.; Sato, K.; Ozeki, Y.; Shinohara, H. Purification and Characterization of Double-Wall Carbon Nanotubes Synthesized by Catalytic Chemical Vapor Deposition on Mesoporous Silica. *Chem*. *Phys*. *Lett*. **2006**, *418*, 408–412.

11. Yang, Y.; Lim, S. Y.; Wang, C.; Du, G.; Haller, G. L. Statistical Analysis of Synthesis of Co-MCM-41 Catalysts for Production of Aligned Single Walled Carbon Nanotubes (SWNT). *Microporous Mesoporous Mater*. **2004**, *74*, 133–141.

12. Lim, S. Y.; Ciuparu, D.; Pak, C.; Dobek, F.; Chen, Y.; Harding, D.; Pfefferle, L.; Haller, G. L. Synthesis and Characterization of Highly Ordered Co−MCM-41 for Production of Aligned Single Walled Carbon Nanotubes (SWNT). *J*. *Phys*. *Chem*. *B* **2003**, *107*, 11048–11056.

13. Mukhopadhyay, K.; Koshio, A.; Sugai, T.; Tanaka, N.; Shinohara, H.; Konya, Z.; Nagy, J. B. Bulk Production of Quasi-Aligned Carbon Nanotube Bundles by the Catalytic Chemical Vapour Deposition (CCVD) Method. *Chem*. *Phys*. *Lett*. **1999**, *303*, 117–124.

14. Noda, S.; Sugime, H.; Osawa, T.; Tsuji, Y.; Chiashi, S.; Murakami, Y.; Maruyama, S. A Simple Combinatorial Method to Discover Co-Mo Binary Catalysts That Grow Vertically Aligned Single Walled Carbon Nanotubes. *Carbon* **2006**, *44*, 1414–1419.

15. Hasegawa, K.; Noda, S. Diameter Increase in Millimeter-Tall Vertically Aligned Single-Walled Carbon Nanotubes during Growth. *Appl*. *Phys*. *Express* **2010**, *3*, 045103–1–3.

16. Hasegawa, K.; Noda, S. Millimeter-Tall Single-Walled Carbon Nanotubes Rapidly Grown with and without Water. *ACS Nano* **2011**, *5*, 975–984.

17. Amama, P. B.; Pint, C. L.; McJilton, L.; Kim, S. M.; Stach, E. A.; Murray, P. T.; Hauge, R. H.; Maruyama, B. Role of Water in Super Growth of Single-Walled Carbon Nanotube Carpets. *Nano Lett*. **2009**, *9*, 44–49.

18. Amama, P. B.; Pint, C. L.; Kim, S. M.; McJilton, L.; Eyinkt, K. G.; Stach, E. A.; Hauge, R. H.; Maruyama, B. Influence of Alumina Type on the Evolution and Activity of Alumina-Supported Fe Catalysts in Single-Walled Carbon Nanotube Carpet Growth. *ACS Nano* **2010**, *4*, 895–904.

19. Structure Commission of the International Zeolite Association. http://www.iza-structure.org/databases/.

20. Moteki, T.; Murakami, Y.; Noda, S.; Maruyama, S.; Okubo, T. Zeolite Surface as a Catalyst Support Material for Synthesis of Single-Walled Carbon Nanotubes. *J. Phys. Chem. C* **2011**, *115*, 24231–24237.

21. Marler, B. On the Relationship between Refractive Index and Density for SiO_2-polymorphs. *Phys. Chem. Minerals* **1988**, *16*, 286–290.

22. Larlus, O.; Valtchev, V. Control of the Morphology of All-Silica BEA-type Zeolite Synthesized in Basic Media. *Chem. Mater.* **2005**, *17*, 881–886

23. Jon, H.; Lu, B.; Oumi, Y.; Itabashi, K.; Sano, T. Synthesis and Thermal Stability of Beta Zeolite Using Ammonium Fluoride. *Microporous Mesoporous Mater.* **2006**, *89*, 88–95.

24. Agger, J. R.; Hanif, N.; Cundy, C. S.; Wade, A. P.; Dennison, S.; Rawlinson, P. A.; Anderson, M. W. Silicalite Crystal Growth Investigated by Atomic Force Microscopy, *J. Am. Chem. Soc.* **2003**, *125*, 830–839.

25. Jorio, A.; Pimenta, M. A.; Souza, A. G.; Saito, R.; Dresselhaus, G.; Dresselhaus, M. S. Characterizing Carbon Nanotube Samples with Resonance Raman Scattering. *New J. Phys.* **2003**, *5*, 139.1–139.17.

26. Jiang, J.; Saito, R.; Sato, K.; Park, J. S.; Samsonidze, Ge. G.; Jorio, A.; Dresselhaus, G.; Dresselhaus, M. S. Chirality dependence of exciton effects in single-wall carbon nanotubes: Tight-binding model. *Phys*. *Rev*. *B* **2007**, *75*, 035407–1–035407–13.

27. Araujo, R. T.; Doorn, S. K.; Kilian, S.; Tretiak, S.; Einarsson, E.; Maruyama, S.; Chacham, H.; Pimenta, M. A.; Jorio, A. Third and Fourth Optical Transitions in Semiconducting Carbon Nanotubes, *Phys*. *Rev*. *Lett*. **2007**, *98*, 067401–1–067401–4.

28. Noda, S. Tsuji, Y.; Murakami, Y.; Maruyama, S. Combinatorial method to prepare metal nanoparticles that catalyze the growth of single-walled carbon nanotubes. *Appl*. *Phys*. *Lett*. **2005**, *86*, 173106–1–173106–3.

29. Telg, H.; Maultzsch, J.; Reich, S.; Hennrich, F.; Thomsen, C. Chirality Distribution and Transtion Energies of Carbon Nanotubes. *Phys*. *Rev*. *Lett*. **2004**, *93*, 177401–1–177401–4.

30. Maultzsch, J.; Telg, H.; Reich, S.; Thomsen, C. Radial breathing mode of single-walled carbon nanotubes: Optical transition energies and chiral-index assignment. *Phys*. *Rev*. *B* **2005**, *72*, 205438–1–205438–16.

31. Telg, H.; Maultzsch, J.; Reich, S.; Thomsen, C. Resonant-Raman intensities and transition energies of the E_{11} transition in carbon nanotubes. *Phys*. *Rev*. *B* **2006**, *74*, 115415–1–115415–5.

32. Dresselhaus, M. D.; Eklund, P. V. Phonons in Carbon Nanotubes. *Adv*. *Phys*. **2000**, *49*, 705–814.

Table of Contents

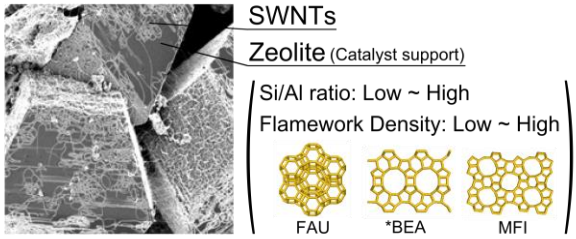

Supporting Information

Influence of Zeolites Catalyst Support on the Synthesis of Single-Walled Carbon Nanotubes: Framework Structures and Si/Al Ratios

Takahiko Moteki,[1] Daiki Nukaga,[1] Yoichi Murakami,[2] Shigeo Maruyama,[3] and Tatsuya Okubo[*,1]

[1]Department of Chemical System Engineering, The University of Tokyo, 7-3-1 Hongo, Bunkyo-ku, Tokyo 113-8656, Japan

[2]Department of Mechanical Sciences and Engineering, Tokyo Institute of Technology, 2-12-1-I1-15 Ookayama, Meguro-ku, Tokyo 152-8552, Japan

[3]Department of Mechanical Engineering, The University of Tokyo, 7-3-1 Hongo, Bunkyo-ku, Tokyo 113-8656, Japan

Contents

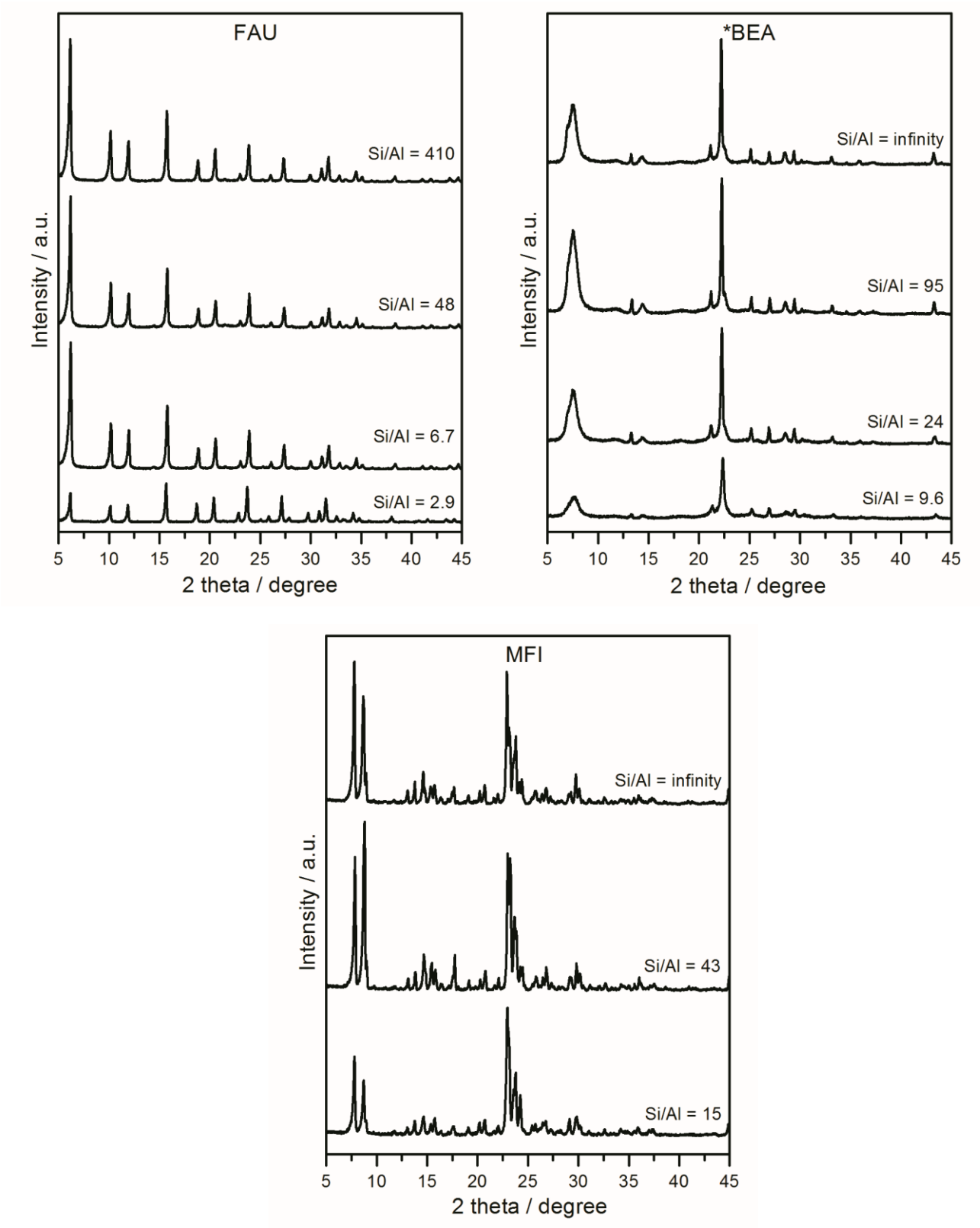

Figure S1. XRD patterns of FAU-, *BEA-, and MFI-type zeolite after pseudo CVD treatments.

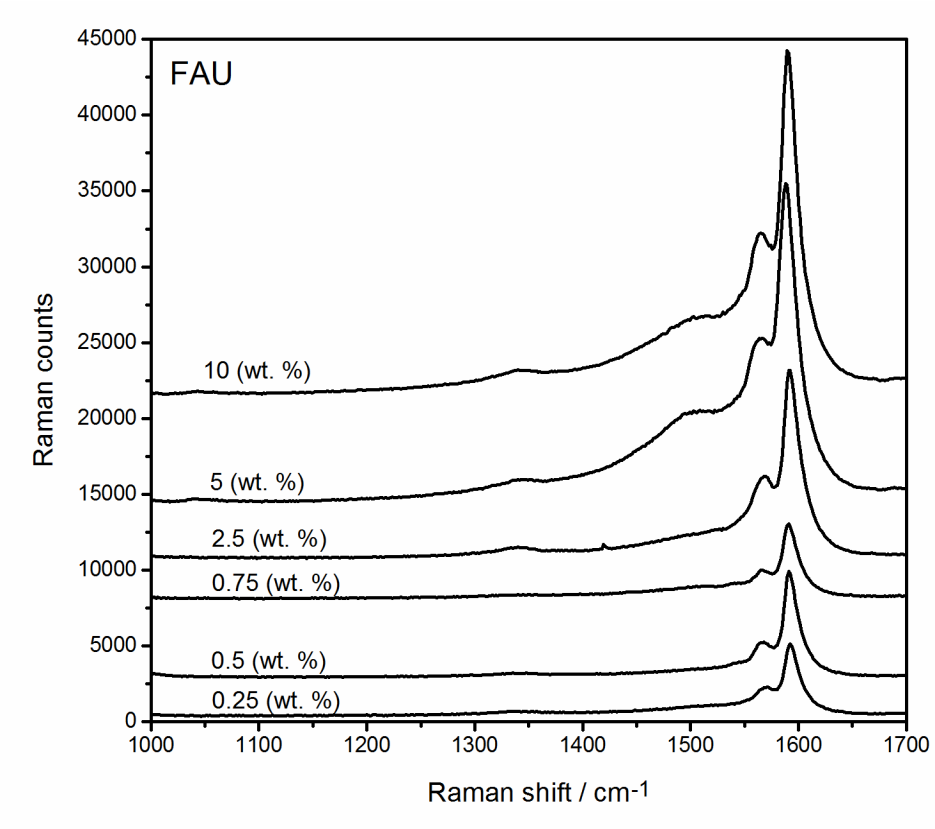

Figure S2(a). Typical Raman spectra of SWNTs synthesized on FAU-type zeolite with Si/Al ratio of 410. The concentration of cobalt acetate varied from 0.1 to 10 wt. %.

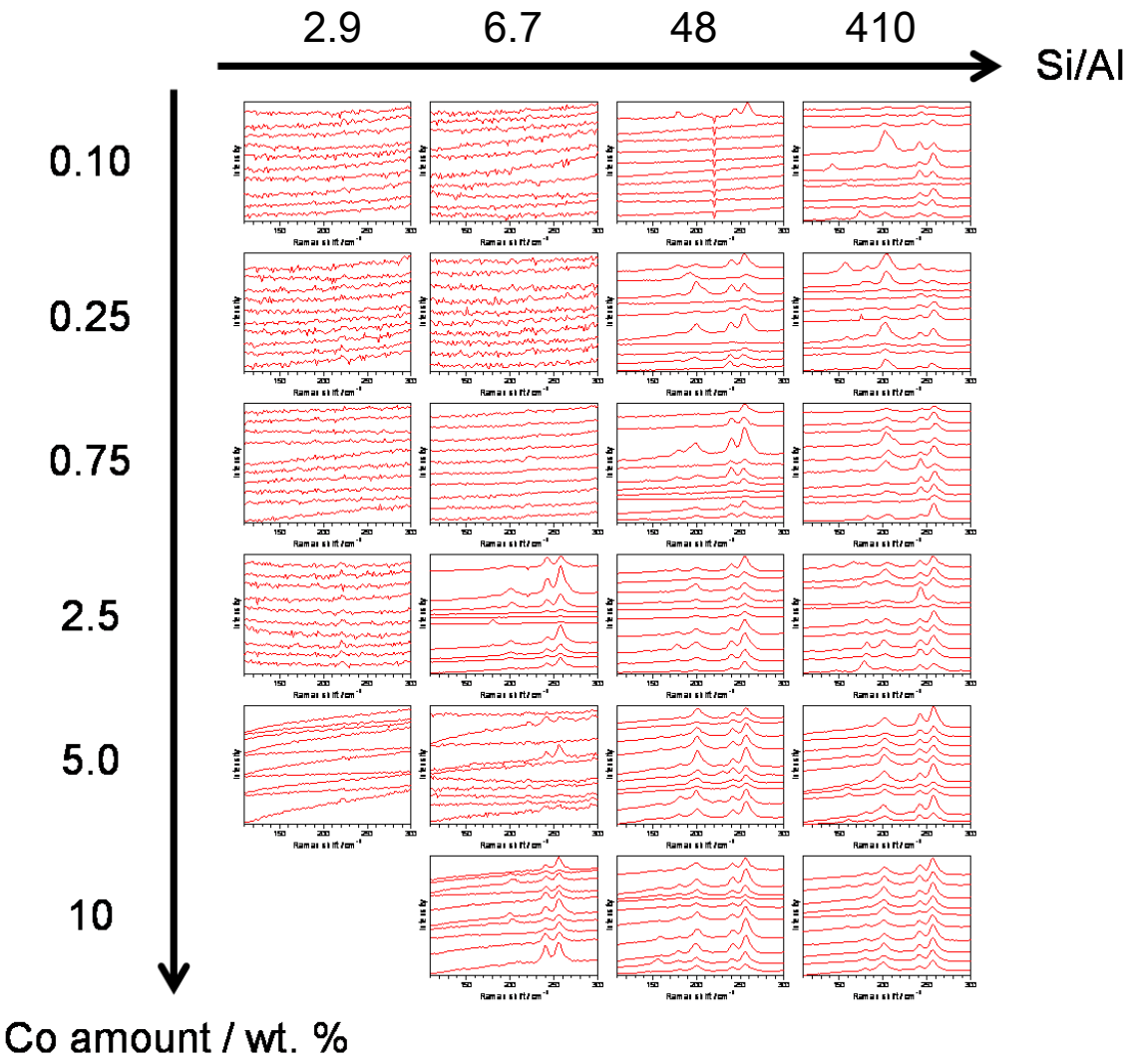

Figure S2(b) RBM spectra of SWNTs synthesized on FAU-type zeolites.

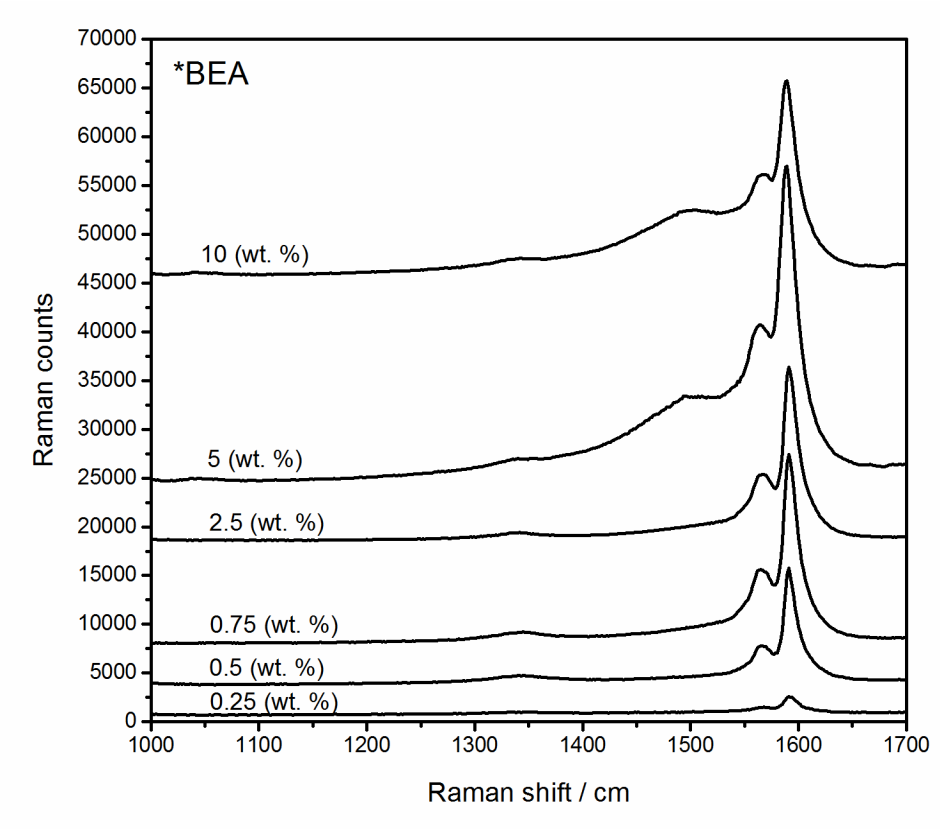

Figure S3(a). Typical Raman spectra of SWNTs synthesized on *BEA-type zeolite with pure silica form. The concentration of cobalt acetate varied from 0.1 to 10 wt. %.

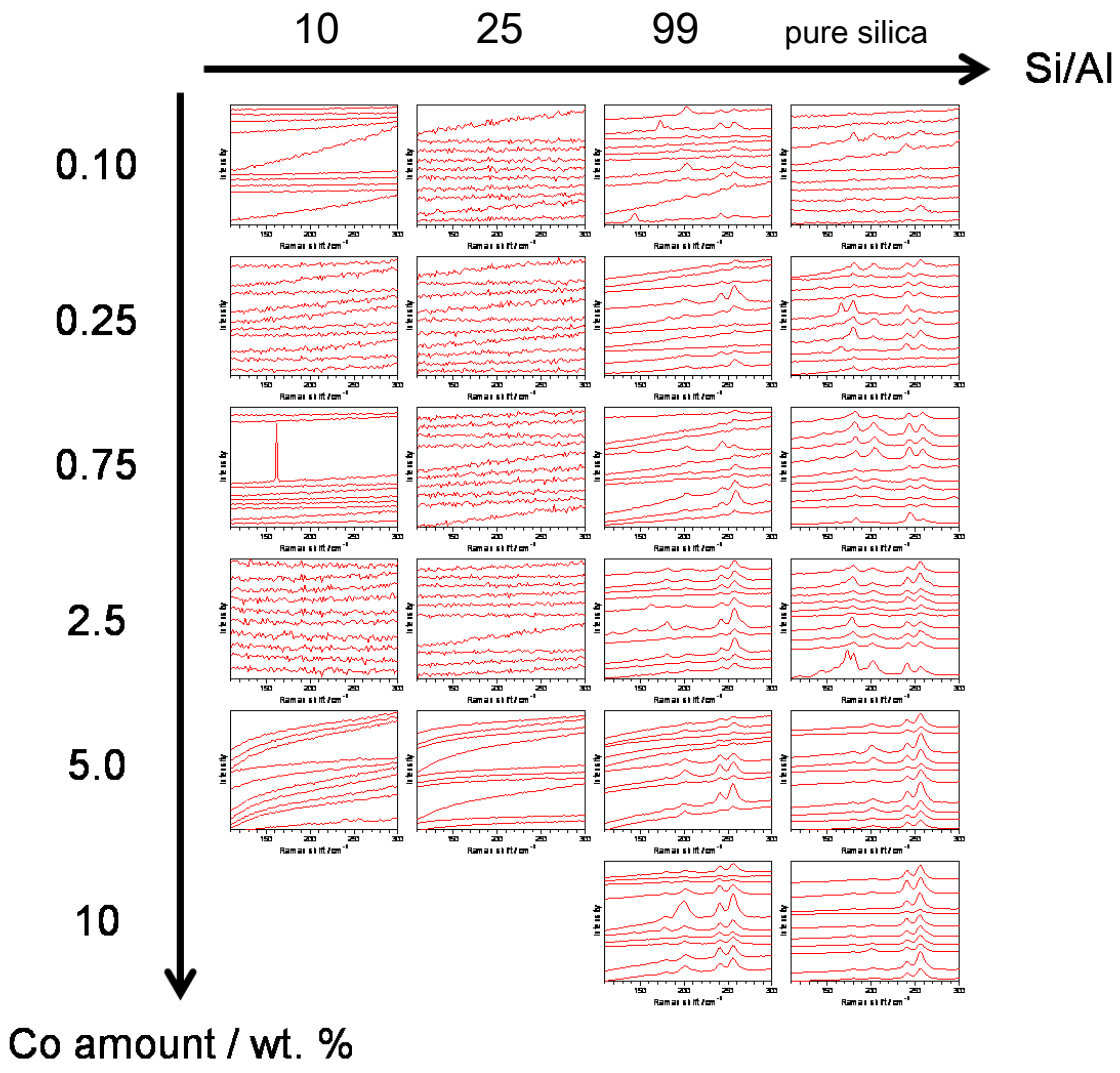

Figure S3(b) RBM spectra of SWNTs synthesized on *BEA-type zeolites.

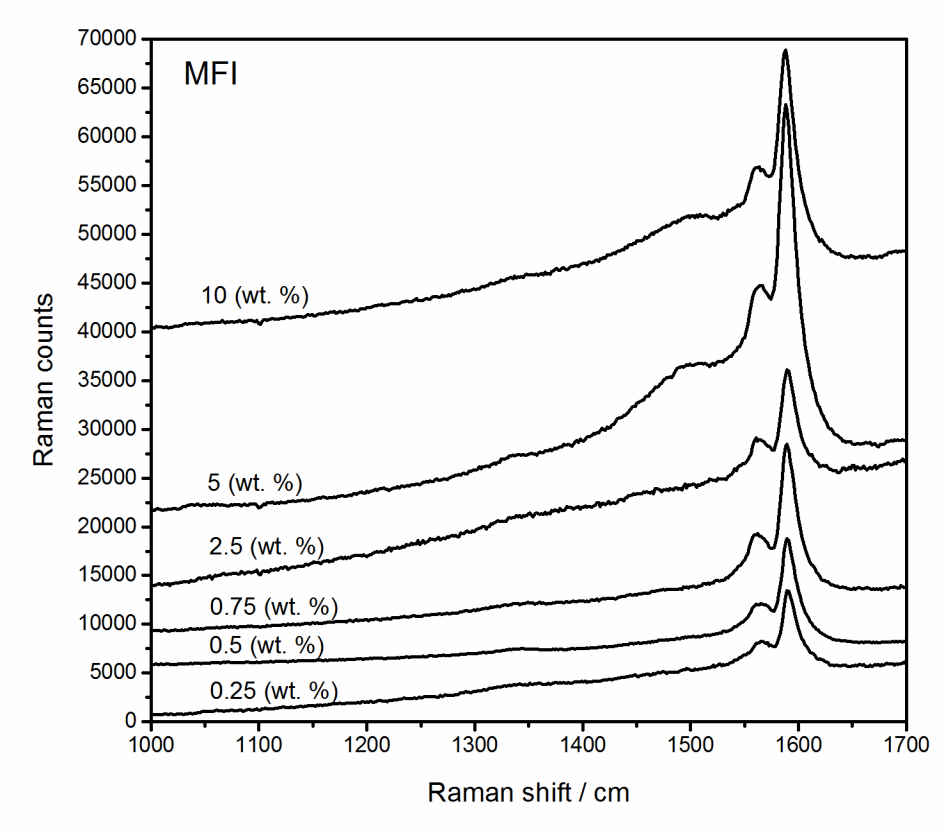

Figure S4(a). Typical Raman spectra of SWNTs synthesized on MFI-type zeolite with pure silica form. The concentration of cobalt acetate varied from 0.1 to 10 wt. %.

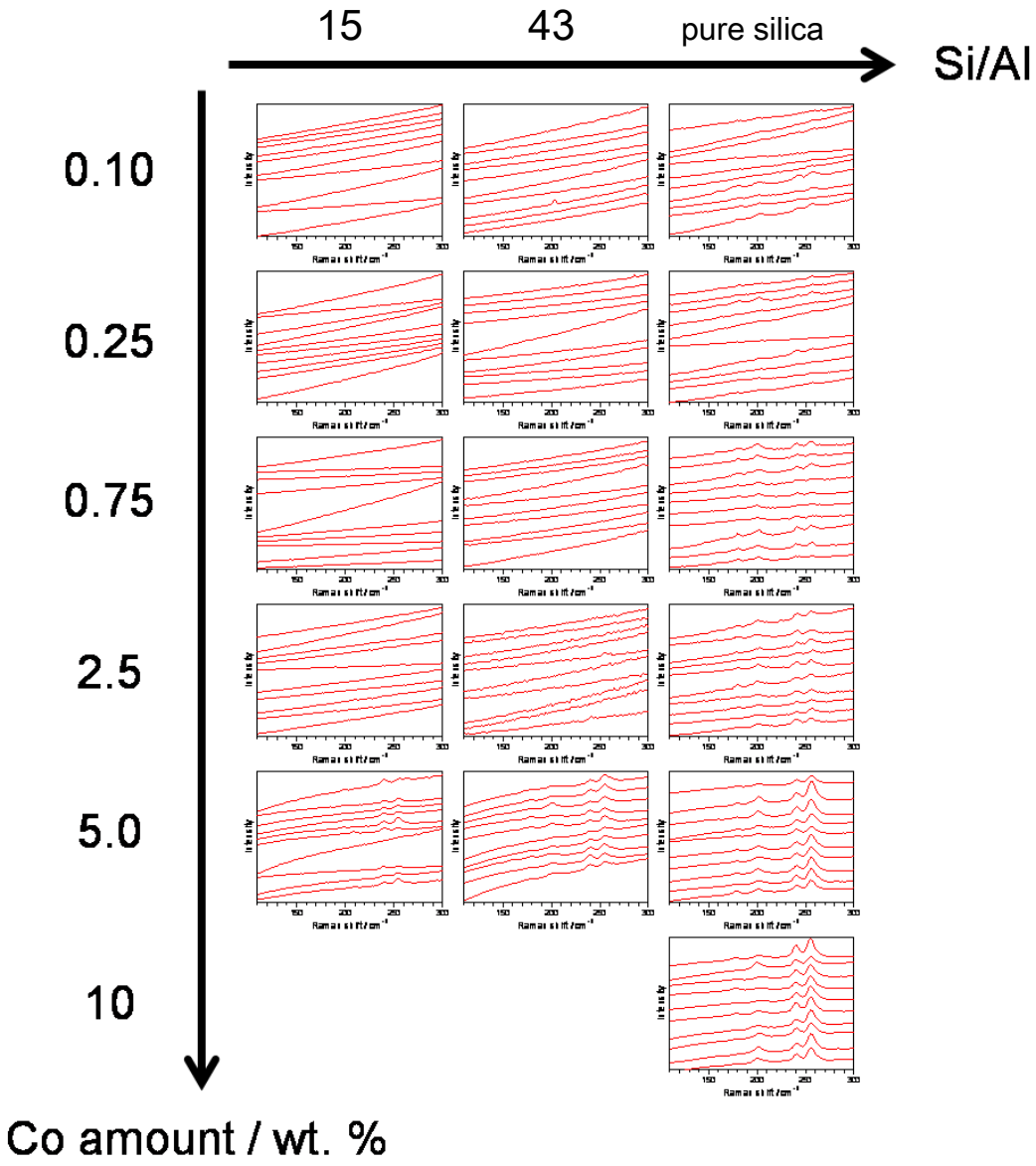

Figure S4(b) RBM spectra of SWNTs synthesized on MFI-type zeolites.